SLAC – PUB – 3940
April 1986
(A)

RF BREAKDOWN STUDIES IN A SLAC DISK-LOADED STRUCTURE*

J. W. WANG, V. NGUYEN-TUONG AND G. A. LOEW
Stanford Linear Accelerator Center
Stanford University, Stanford, California 94305

Summary

RF breakdown studies in an S-band standing-wave disk-loaded accelerator structure have been completed. An equivalent traveling-wave accelerating gradient as high as 147 MV/m and a peak field in excess of 300 MV/m have been obtained. At these high gradients, considerable amounts of field emission and x-ray radiation are observed. Some of the field-emitted electrons are captured and focused by the RF fields and can be extracted on the axis of the structure. Their current, energy distribution and the x-ray radiation they produce are given. RF processing as measured by the frequency of breakdown and the reduction in field emitted electron currents inside the structure can be speeded up considerably by the presence of argon. Some conjectures on the causes of breakdown are presented.

Discussion of Early Results

The study of accelerator structures under high-gradient conditions which is reported here started at SLAC in late 1983. A first status report on this work was presented at the 1985 Particle Accelerator Conference.[1] All the experimental results were obtained with a $2\pi/3$, seven cavity disk-loaded standing-wave (SW) section made from a segment of standard SLAC traveling-wave (TW) structure capped off at one end. Its dimensions and properties calculated by SUPERFISH for a 1-1/2 cavity cell are recapitulated in Table 1.

Table 1. Fields calculated for normalizing condition $|\int_0^L E_z(z)\,e^{j(\omega z/c)}dz\,|\,/L = 1$ MV/m.

Length of seven cavities	24.5 cm
Iris diameter $2a$	1.99 cm
Cavity diameter $2b$	8.19 cm
Traveling-wave r/Q per unit length	45.5 Ω/cm
Q	13,793
Resonant frequency f	2856 MHz
Standing-wave R/Q for length $L = 5.25$ cm	119.5 Ω
$\|\int_0^L E_z(z)e^{j(\omega z/c)}dz\|$	0.0525 MV
Energy stored W	1.239×10^{-3} J
Power dissipated $P_D = \omega W/Q$	1611.7 W
Max. axial field at $z = 0$, $\|E_{z,SW}\|_{max}$	2.692 MV/m
Max. surface field at disk edge, $\|E_{s,SW}\|_{max}$	4.263 MV/m
Average accelerating field $\bar{E}_{acc}$	0.9815 MV/m
$\|E_{z,SW}\|_{max}/\bar{E}_{acc}$	2.742
$\|E_{s,SW}\|_{max}/\bar{E}_{acc}$	4.342

Note that some of the entries into this table are different from those in Ref. 1 because of minor changes in interpretation of the SUPERFISH output. As a result, the revised equivalent TW fields for a power input P_{in} in MW are:

$$E_{z,TW} = \sqrt{P_{in}/18.05} \times 100 \text{ MV/m} \qquad (1a)$$

$$E_{s,TW} = \sqrt{P_{in}/18.05} \times 217 \text{MV/m} \quad . \qquad (1b)$$

After proper matching and tuning, the resonant section was gradually RF processed at increasing power levels during Spring 1984 and yielded equivalent TW accelerating fields $E_{z,TW}$ of ~ 129 MV/m and corresponding surface fields $E_{s,TW}$ of ~ 281 MV/m for 2.5 μsec pulses at a peak power input of 30.2 MW. After several experimental modifications but before the klystron power could be increased further, a second series of tests was started in Spring 1985. In the course of these tests, considerable field emission current and x-ray radiation were observed and an unexpected accident took place. In the scenario as we have reconstructed it, after the section was perhaps processed insufficiently or too rapidly, the equivalent of roughly 1 μA average of field emitted current was captured and focused by the RF fields (an equivalent of about 3 kG axial magnetic field) onto the stainless steel end-plate and punctured a 1 mm diameter hole through it by melting and implosion. This caused the section to go up to air and three or four disks to be covered with a thin coat of stainless steel. Fortunately, no Q degradation could be measured.

New Experimental Results

Before resuming our measurements, several improvements were made in the experimental set-up.

The two stainless steel end-plates were replaced with half-inch thick copper plates thinned down to round 0.015 inch (0.38 mm)thick windows, 1.4 cm in diameter, to permit extraction and analysis of the field emitted beam. The downstream window and two SMA connectors and probes are shown in Fig. 1 together with a sketch of the section. A Faraday cup was installed coaxially downstream of the section to measure the straight-ahead emitted beam current.

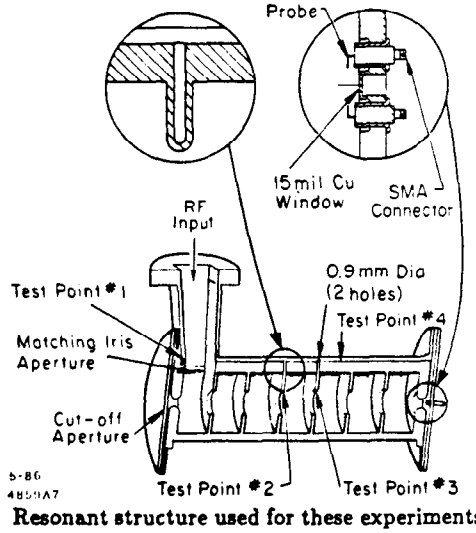

Fig. 1. Resonant structure used for these experiments. Numbered test points indicate locations of thermocouples to monitor temperatures during operation. End-plate shows thin window and probes.

The vacuum system was equipped with an additional leak valve and two gas inlet valves to inject controllable amounts of argon or nitrogen gas into the structure in order to study RF processing under various gas and pressure conditions. A 7 db directional coupler was removed from the klystron output

*Work supported by the Department of Energy, contract number DE-AC03-76SF00515.

Contributed to the Stanford Linear Accelerator Conference, Stanford, California, June 2-6, 1986

waveguide system to increase the peak power to the section up to 40 MW. A simple spectrometer was installed to measure the energy spectrum of the beam emerging from the section and transmitted through a slit to a lead brick collector (see Fig. 4). Several small ion chambers were calibrated to monitor the x-ray radiation level at various coordinates around the section, and an x-ray pin-hole camera was constructed to look at where the radiation originated in the section.

After the section was gradually RF processed under vacuum for a number of hours, the following very repeatable gradient limits were reached, above which breakdown invariably occurred:

Table 2.

Pulse length (μsec)	2.5	1.5
P_{in} (MW)	37.3	38.8
$E_{z,TW}$ (MV/m)	143.8	146.7
$E_{s,TW}$ (MV/m)	312	318

These results show that within the small range of observation, the breakdown limit is not a strong function of pulse length. Note that the cavity filling time is roughly 0.5 μsec. The breakdown behavior suggests that a fairly abrupt "brick wall" is reached at these levels. Some possible interpretations of this phenomenon will be offered later in the paper.

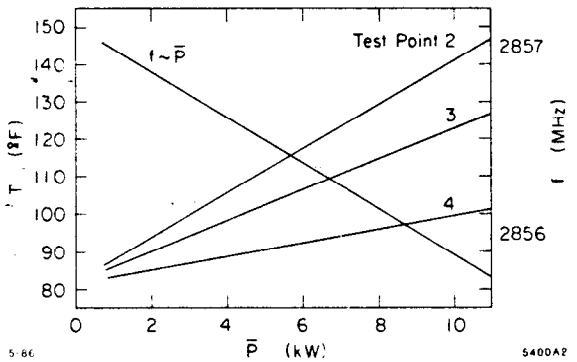

Fig. 2. Temperatures for the test points shown in Fig. 1 and resonant frequency, both as a function of average power dissipated in accelerator section.

The average power $\bar{P}$ to the section was increased up to 10 kW at 120 pps. Figure 2 gives the temperature measured at various test points shown in Fig. 1 and the resonant frequency as a function of the average power dissipated in the section. The linear variations, repeatable from measurement to measurement, indicate that the deformations of the section caused by heat in this range are not permanent.

The cross-section of the field emitted beam was measured with a piece of cinemoid film placed on both upstream and downstream outside surfaces of the windows and found to be approximately 3 mm in diameter, almost independently of RF power level. The beam current transmitted through the downstream window was measured with the Faraday cup and found to reach 25 mA peak at 35 MW peak power, as shown in Fig. 3. By passing through the window, the electrons produce an electromagnetic shower and are scattered at various energies and angles. The relative beam current transmitted to the beam collector behind the slit formed by two lead bricks (see Fig. 4) was measured as a function of the spectrometer setting

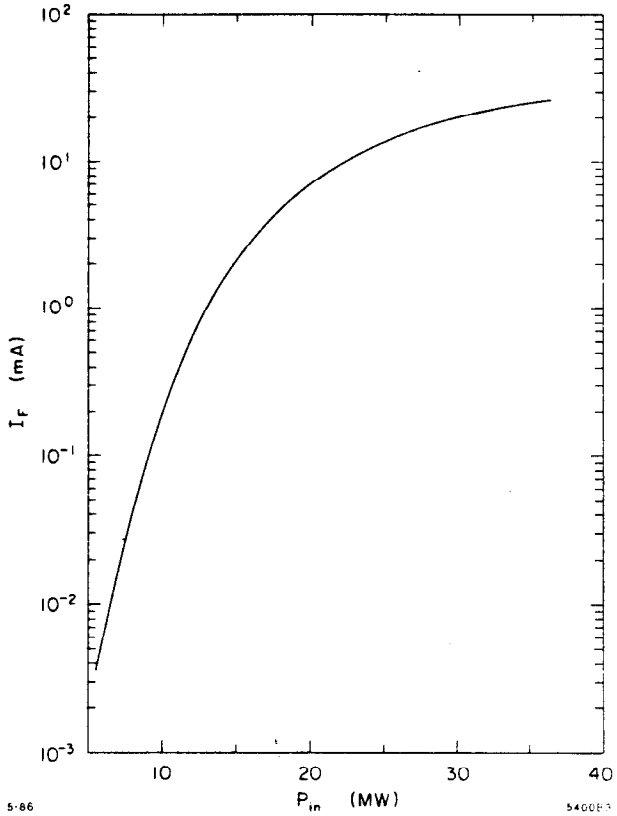

Fig. 3. Field emitted beam current transmitted through downstream (right-hand side in Fig. 1) window to Faraday cup as a function of peak input power.

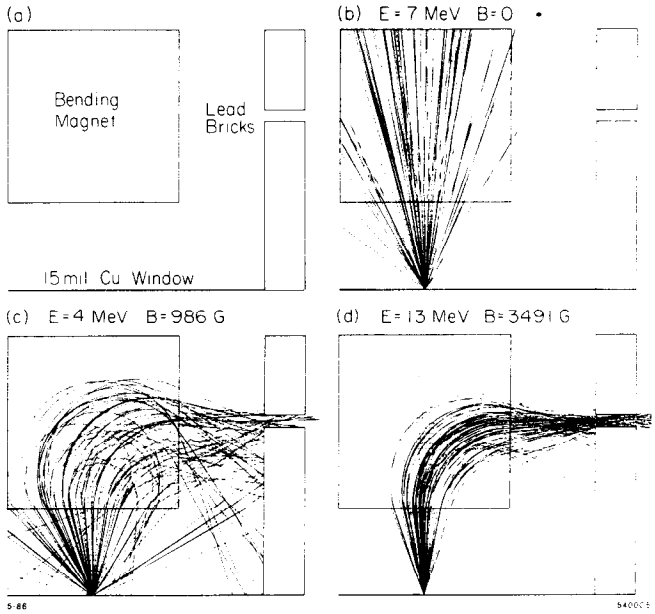

Fig. 4. (a) Layout of window, spectrometer magnet and slit; (b), (c) and (d) Electron trajectories (continuous lines) and γ-rays (dotted lines) for various initial electron energies and magnetic fields.

between 0 and 4000 G to give energy spectra for various power levels. These energy spectra had to be corrected for scattering through the window and gas scattering. This was done with the aid of the program EGS 4 which simulates bremstrahlung, electron-electron scattering, ionization loss, pair production,

photoelectric effect and multiple Coulomb scattering, and TRANSPORT. For each incident electron energy and corresponding magnetic field for maximum transmission through the slit, a ratio of current to the collector to current incident on the window could be obtained (see the various examples of Fig. 4). This ratio was then used to renormalize the measured spectra at various power levels and obtain the actual electron spectra (see Fig. 5). The double humps correspond to electrons captured in the third cavity and accelerated through the entire section or captured in the sixth cavity and accelerated to the output end. The extremely elevated x-ray dosage distribution is shown in Fig. 6.

Figure 7 shows a typical RF processing sequence as illustrated by a series of Fowler-Nordheim plots. These plots are based on the model that the field emission current $\bar{I}_F$ is caused by conduction electrons tunneling through a potential barrier under the influence of an external macroscopic surface field E enhanced by a factor β:

$$\frac{\bar{I}_F}{E^{2.5}} = \frac{C}{f^2} \exp\left(\frac{-1.34 \times 10^{10}\phi^{1.5}}{\beta E}\right) \qquad (2)$$

where $\bar{I}_F$ is measured in amperes, E in volts/m, f is the RF frequency, ϕ is the work function in electron volts, and C is a constant. The formula[2] has been corrected to take into account the averaging effect over an RF cycle due to the time-dependent nature of the barrier. When displayed on a log-log plot, the slope of the straight lines yields the value of β. Line (1) corresponds to some fairly arbitrary starting condition after the section had been baked to 250° C for several hours. Line (2) corresponds to a time, several weeks later, after considerable amount of RF processing had taken place. Line (3) shows the condition obtained after careful RF processing has been done in the presence of argon at 10^{-5} Torr with an input power of 9.3 MW at 120 pps for about sixty minutes. Line (4) was obtained the next day after the argon had been pumped out and the vacuum was 3×10^{-8} Torr. Note the successive reductions in the value of β from 140 down to 102.

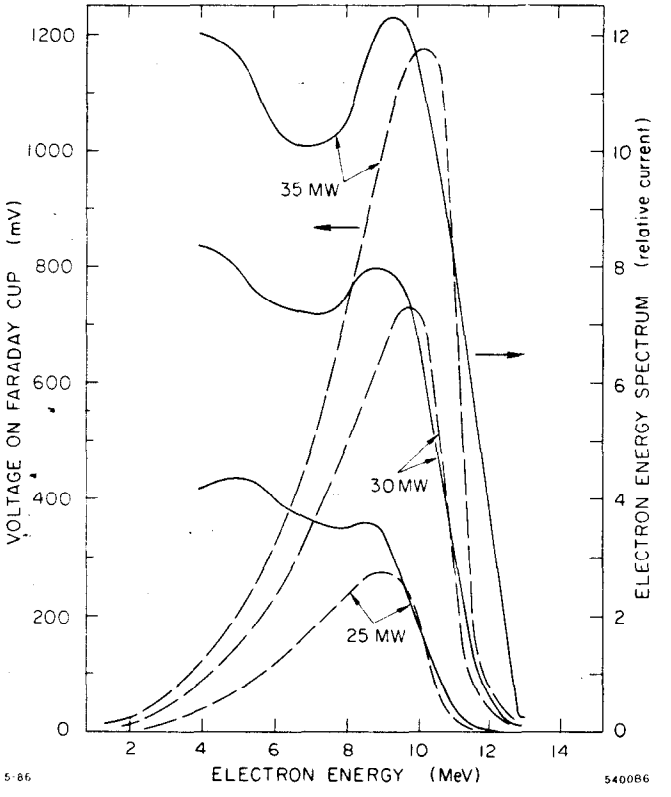

Fig. 5. Uncorrected (continuous lines) and corrected (dashed lines) electron energy spectra for various values of peak input power.

Argon processing appears to be a quick method to decrease field emission and push up the breakdown limit. However, field emission, sudden changes in the value of β and the argon pressure must be monitored very carefully. For example, in one test we set the argon pressure to 10^{-4} Torr and found that the value of β actually increased.

Discussion and Conjectures

The breakdown limits given in this paper represent only one point at one RF frequency. They seemed to be very reproducible, thus giving the impression of a hard "brick wall" limit. The interpretation of the value of β has to be qualified. Originally, in the study of field emission, the enhancement was believed to be caused by whiskers or microprotrusions. Subsequently, other causes have been advanced, such as oxide films and associated trapped positive charges, partially embedded non-metallic impurities, or other forms of contamination. Some authors (see for example Ref. 3) have reported DC breakdown thresholds at levels on the order of 7 GV/m and attributed them to ohmic and Nottingham-effect heating and vaporization of microprotrusions. If we assume the β of

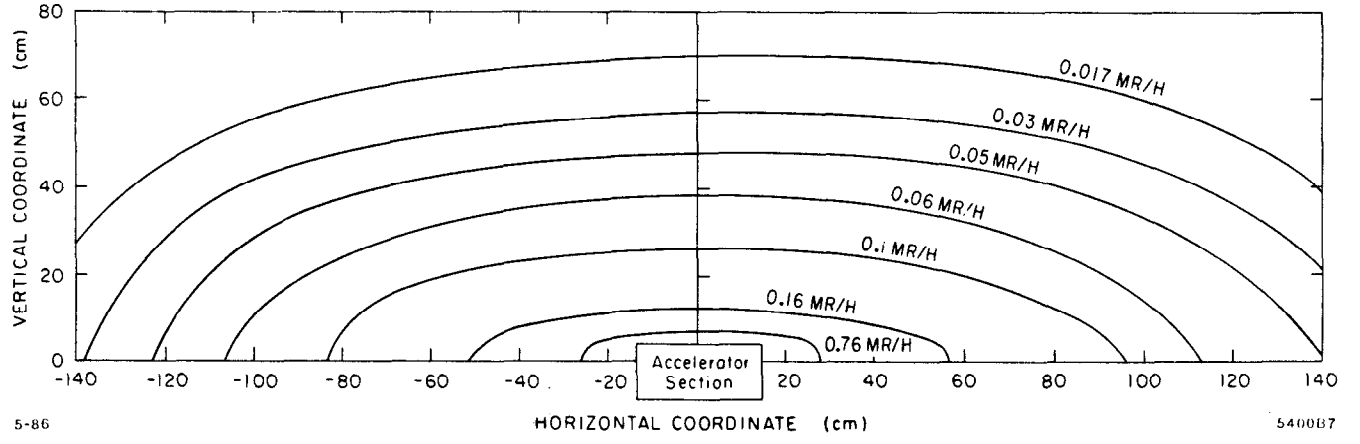

Fig. 6. X-ray dosage distribution around accelerator section (300 MV/m surface field, 2.5 μsec, 120 pps).

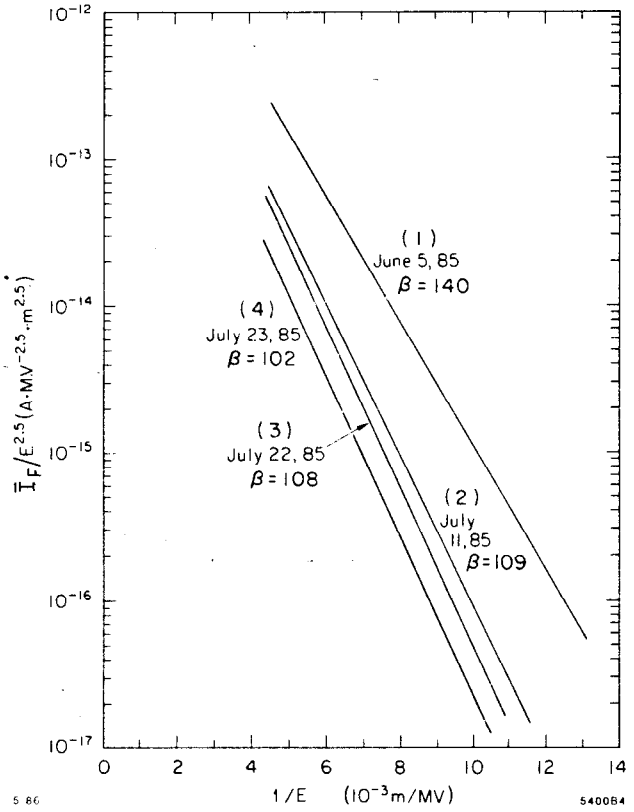

Fig. 7. Modified Fowler-Nordheim plots.

~ 100 which we measured to be entirely geometrical, then the breakdown corresponding to 300 MV/m would have happened at 30 GV/m which is four times higher than the above DC breakdown of 7 GV/m. On the other hand, if one were looking for a totally catastrophic effect, one might theorize that since the ionization potential of copper is 7.6 eV, at the Bohr radius of 0.528×10^{-11} m it would take ~ 150 GV/m to pull off all electrons from the metal surface, yet another factor of five higher. At this juncture, we are left with a number of uncertainties and questions: what is really taking place physically at our 300 MV/m breakdown threshold? If we just have a few microprotrusions or embedded impurities, why can't we vaporize them and move on to higher fields? Does the elimination of one mountain create another mountain next to it? Or, do we have such a large number of them that we can never get rid of all of them? Clearly, more experiments are needed to answer these questions and shed more light on the underlying physics.

Acknowledgements

The authors wish to thank R. H. Miller, R. McCall, R. Nelson, K. Brown and J. Zamzow for useful discussions and assistance in some of the experiments.

References

1. J. W. Wang and G. A. Loew, Measurements of Ultimate Accelerating Gradients in the SLAC Disk-Loaded Structure, IEEE Trans. on Nucl. Sci., **NS-32**, October 1985.
2. J. W. Wang, private communication.
3. H. A. Schwettman, J. P. Turneaure, and R. F. Waites, Evidence for Surface-State-Enhanced Field Emission in RF Superconducting Cavities, Jour. Appl. Phys., **Vol. 45**, No. 2, February 1974.